The Mechanism of the Slippage Approach to Rotaxanes. Origin of the "All-or-Nothing" Substituent Effect†

Françisco M. Raymo, K. N. Houk,* and J. Fraser Stoddart*

Contribution from the Department of Chemistry and Biochemistry, University of California, 405 Hilgard Avenue, Los Angeles, California 90095-1569

Received February 24, 1998. Revised Manuscript Received June 25, 1998

Abstract: Heating a solution of the circular bis-*p*-phenylene-34-crown-10 and a dumbbell-shaped bipyridinium component, terminated at both ends by 4-*R*-phenyl-bis(4-*tert*-butyl-phenyl)methane-based stoppers, affords the corresponding [2]rotaxane when *R* is equal to H, Me, and Et, following the slippage of the macrocycle over the stoppers of the dumbbell. By contrast, no [2]rotaxane is obtained when *R* is equal to *i*-Pr. Computational investigations with the AMBER* force field provide an explanation of this dramatic substitutent effect. The phenomenon was simulated by the passage of the bis-*p*-phenylene-34-crown-10 macrocycle over four 4-*R*-phenyl-bis(4-*tert*-butyl-phenyl)methane model stoppers. For *R* equal to H, Me, Et, and *i*-Pr, there are two main energy barriers which have to be surpassed in order to permit the passage of the macrocycle over the bulky stoppers. When *R* is equal to H or Me, the rate-determining step is the passage of the macrocycle over a *t*-Bu-C_6H_4- ring. By contrast, when *R* is equal to Et or *i*-Pr, the rate-determining step becomes the passage of the macrocycle over the *R*-C_6H_4- ring. However, when *R* is equal to *i*-Pr, the resulting energy barrier is more than 21 kcal mol^{-1} higher than in the case of any of the other stoppers. These results are in good agreement with the experimental observations and provide a quantitative explanation for the rigorous size complementarity requirements between macrocycle and stopper which have been observed experimentally.

Introduction

The so-called slippage[1] approach has been employed successfully in our laboratories to self-assemble[2] a series of linear[1a−c,e−g] and branched[1d,h] [*n*]rotaxanes[3] incorporating a bipyridinium-based backbone, encircled by one or more dioxyarene-based macrocyclic components. In one instance, a linear [3]rotaxane,[1c,f,g] incorporating two constitutionally different macrocyclic components, has also been obtained as a result of slippage. A kinetic investigation of the slippage processes revealed[1f,g] that the free energies of activation associated with the slipping-on and slipping-off processes (Figure 1) are correlated with the size of the cavity of the macrocyclic component, as well as with the size of the stoppers attached to both ends of the dumbbell-shaped component. The free energies of activation increase upon reducing the size of the cavity of the macrocyclic component and/or enlarging the bulk of the stoppers. As a result, the isolated yields of the [2]rotaxanes are affected profoundly by subtle chemical changes, as illustrated in the example shown in Figure 1, where the *R* group attached to one of the phenyl rings of the tetraarylmethane-based stoppers, is varied systematically. Heating a MeCN solution of the π-electron rich macrocycle bis-*p*-phenylene-34-crown-10 (**BPP34C10**) and one of the π-electron deficient dumbbell-shaped compounds shown in Figure 1 at 55 °C for 10 days afforded[1a,e] the corresponding [2]rotaxanes in yields of 52, 45, and 47% when *R* is H, Me, and Et, respectively. On the contrary, when *R* is an *i*-Pr group, no [2]rotaxane was isolated[1a,e] under otherwise identical conditions; an "all-or-nothing" substituent effect is observed on going from Et to *i*-Pr!

* Correspondence address: Professor K. N. Houk & J. F. Stoddart, Department of Chemistry and Biochemistry, University of California, 405 Hilgard Avenue, Los Angeles, CA 90095-1569. Fax: (310) 206-1843. E-mail: houk@chem.ucla.edu. E-mail: stoddart@chem.ucla.edu.

† Molecular Meccano, Part 40. For Part 39, see: Ashton, P. R.; Fyfe, M. C. T.; Martínez-Díaz, M. V.; Menzer, S.; Schiavo, C.; Stoddart, J. F.; White A. J. P.; Williams, D. J. *Chem. Eur. J.* **1998**, *4*, 1523−1534.

(1) (a) Ashton, P. R.; Belohradsky, M.; Philp, D.; Stoddart, J. F. *J. Chem. Soc., Chem. Commun.* **1993**, 1269−1274. (b) Ashton, P. R.; Belohradsky, M.; Philp, D.; Spencer, N.; Stoddart, J. F. *J. Chem. Soc., Chem. Commun.* **1993**, 1274−1277. (c) Amabilino, D. B.; Ashton, P. R.; Belohradsky, M.; Raymo, F. M.; Stoddart, J. F. *J. Chem. Soc., Chem. Commun.* **1995**, 747−750. (d) Amabilino, D. B.; Ashton, P. R.; Belohradsky, M.; Raymo, F. M.; Stoddart, J. F. *J. Chem. Soc., Chem. Commun.* **1995**, 751−753. (e) Ashton, P. R.; Ballardini, R.; Balzani, V.; Belohradsky, M.; Gandolfi, M. T.; Philp, D.; Prodi, L.; Raymo, F. M.; Reddington, M. V.; Spencer, N.; Stoddart, J. F.; Venturi, M.; Williams, D. J. *J. Am. Chem. Soc.* **1996**, *118*, 4931−4951. (f) Asakawa, M.; Ashton, P. R.; Ballardini, R.; Balzani, V.; Belohradsky, M.; Gandolfi, M. T.; Kocian, O.; Prodi, L.; Raymo, F. M.; Stoddart, J. F.; Venturi, M. *J. Am. Chem. Soc.* **1997**, *119*, 302−310. (g) Raymo, F. M.; Stoddart, J. F. *Pure Appl. Chem.* **1997**, *69*, 1987−1997. (h) Amabilino, D. B.; Asakawa, M.; Ashton, P. R.; Ballardini, R.; Balzani, V.; Belohradsky, M.; Credi, A.; Higuchi, M.; Raymo, F. M.; Shimizu, T.; Stoddart, J. F.; Venturi, M.; Yase, K. *New J. Chem.* **1998**, 959−972.

(2) (a) Lindsey, J. S. *New J. Chem.* **1991**, *15*, 153−180. (b) Whitesides, G. M.; Mathias, J. P.; Seto, C. T. *Science* **1991**, *254*, 1312−1319. (c) Whitesides, G. M.; Simanek, E. E.; Mathias, J. P.; Seto, C. T.; Chin, D. N.; Mammen, M.; Gordon, D. M. *Acc. Chem. Res.* **1995**, *28*, 37−44. (d) Lawrence, D. S.; Jiang, T.; Levett, M. *Chem. Rev.* **1995**, *95*, 2229−2260. (e) Raymo, F. M.; Stoddart, J. F. *Curr. Opin. Colloid Interface Sci.* **1996**, *1*, 116−126. (f) Philp, D.; Stoddart J. F. *Angew. Chem., Int. Ed. Engl.* **1996**, *35*, 1154−1196. (g) Fyfe, M. C. T.; Stoddart, J. F. *Acc. Chem. Res.* **1997**, *30*, 393−401. (e) Gillard, R. E.; Raymo, F. M.; Stoddart, J. F. *Chem. Eur. J.* **1997**, *3*, 1933−1940. (h) Raymo, F. M.; Stoddart, J. F. *Curr. Opin. Colloid Interface Sci.* **1998**, *3*, 150−159.

(3) (a) Dietrich-Buchecker, C. O.; Sauvage J.-P. *Bioorg. Chem. Front.* **1991**, *2*, 195−248. (b) Gibson, H. W.; Marand, H. *Adv. Mater.* **1993**, *5*, 11−21. (c) Chambron, J. C.; Dietrich-Buchecker, C. O.; Sauvage, J.-P. *Top. Curr. Chem.* **1993**, *165*, 131−162. (d) Gibson, H. W.; Bheda, M. C.; Engen, P. T. *Prog. Polym. Sci.* **1994**, *19*, 843−945. (e) Amabilino, D. B.; Parsons, I. W.; Stoddart, J. F. *Trends Polym. Sci.* **1994**, *2*, 146−152. (f) Amabilino, D. B.; Stoddart, J. F. *Chem. Rev.* **1995**, *95*, 2725−2828. (g) Raymo, F. M.; Stoddart, J. F. *Trends Polym. Sci.* **1996**, *4*, 208−211. (h) Belohradsky, M.; Raymo, F. M.; Stoddart, J. F. *Collect. Czech. Chem. Commun.* **1996**, *61*, 1−43. (i) Belohradsky, M.; Raymo, F. M.; Stoddart, J. F. *Collect. Czech. Chem. Commun.* **1997**, *62*, 527−557.

S0002-7863(98)00622-2 CCC: $15.00
Published on Web 08/28/1998

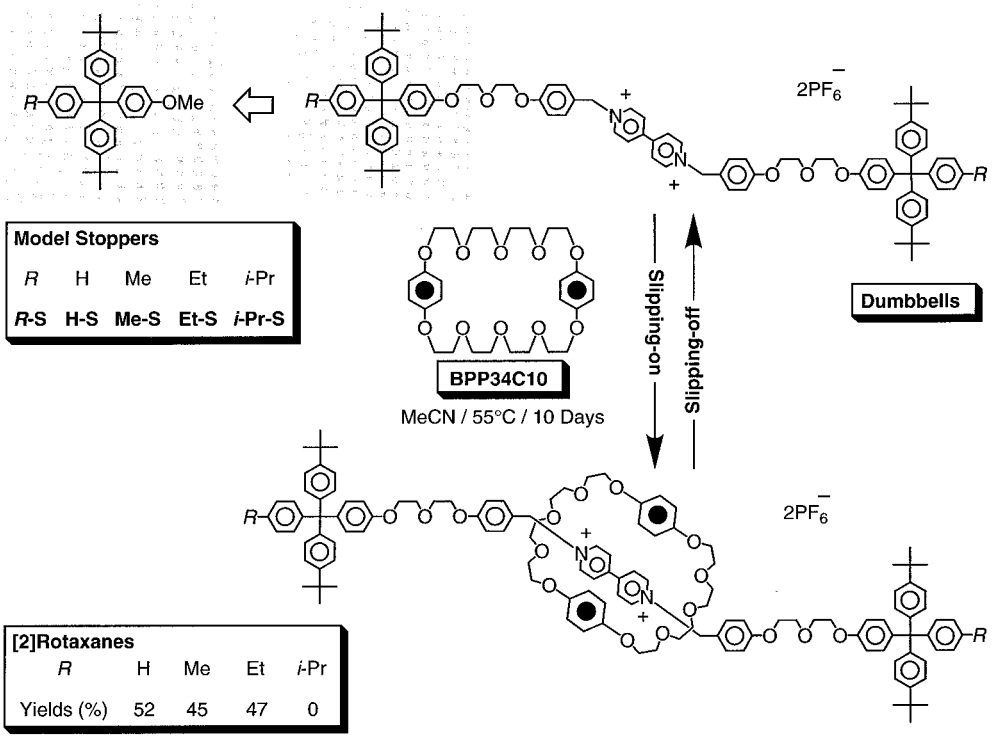

Figure 1. Experimental yields for the rotaxane formation as a result of slippage. The model stoppers employed in the computational simulations are shown in the box in the upper left corner.

To understand the origin of this abrupt shut-down of the slippage process, we have undertaken a computational investigation employing the **BPP34C10** macrocycle and the tetraarylmethane-based model stoppers ***R*-S** illustrated in Figure 1 [***R*** indicates the nature of the *R* group (H, Me, Et, or *i*-Pr), while **S** stands for stopper].

Results and Discussion

Method. In the slipping-on process (Figure 1), the **BPP34C10** macrocycle can approach, at least in principle, the tetraarylmethane-based stoppers from any direction in space. By contrast, in the slipping-off process, the **BPP34C10** macrocycle approaches the stoppers from one direction only by "sliding" along the axis of the threadlike portion of the dumbbell-shaped component. Subsequently, four different pathways can be envisaged, (i) simultaneous passage of the three aryl rings through the cavity of the macrocycle, (ii) simultaneous passage of two aryl rings followed by the slippage of the remaining aryl ring, (iii) slippage of one aryl ring followed by the simultaneous passage of the remaining two aryl rings, or (iv) consecutive three-step passage of the three aryl rings. The average distances between the two *t*-Bu substituents and between the *R* group and one of the two *t*-Bu substituents of each stopper exceed the maximum width of **BPP34C10** (calculated as the separation between the van der Waals surfaces of the central oxygen atoms of the two polyether chains) by at least 1 Å. Thus, the simultaneous passage of three or even two aryl rings through the cavity of **BPP34C10** is not possible without major distortion of the macrocyclic polyether cavity. The slipping-off process can only occur via a three-step pathway involving the passage of a single aryl ring through the cavity of the macrocycle at each step. Any of these steps could be rate-determining, but only if one aryl substituent is enormously large would the passage of the last group be rate-determining. As found in this study, the passage of either the first or the second aryl ring can be rate-determining in these systems.

Because the transition states of both the slipping-on and slipping-off processes must be the same, we searched for the transition state of the slipping-off process. To reduce the computational time, the tetraarylmethane-based model compounds ***R*-S** shown in Figure 1 were employed. The four model compounds ***R*-S** were constructed within the input mode of Macromodel[4] 5.0 and then subjected individually to energy minimization using the Polak-Ribiere conjugate gradient (PRCG) algorithm.[5] The AMBER* force field[6] with the GB/SA H_2O model[7] to resemble a polar solvent was used. The initial geometries[8] shown in Figure 2 were chosen. In each case, a "dummy" atom was placed at a distance of 60.0 Å from the oxygen atom of the methoxy group of the stopper ***R*-S**, and the coordinates of both dummy and oxygen atoms were fixed, employing a force constant of 9999 kJ mol^{-1} $Å^{-2}$ and a half-width restraint of 0.0 Å. The distances *D* between the dummy atom and the carbon atoms of the **BPP34C10** highlighted in Figure 2 were varied in steps from 58.0 to 35.0 Å. At each step, an energy minimization was performed, employing the output structure of one step as the input structure for the subsequent step. The distances *D* were varied by 1.0 Å at each step from 58.0 to 56.0 Å and from 49.0 to 35.0 Å, while the step size was reduced to 0.2 Å from 56.0 to 49.0 Å, the region of the transition state. The energy profiles determined in this way showed evidence of significant hysteresis (see later), and

(4) Mahamadi, F.; Richards, N. G. K.; Guida, W. C.; Liskamp, R.; Lipton, M.; Caufield, D.; Chang, G.; Hendrickson, T.; Still, W. C. *J. Comput. Chem.* **1990**, *11*, 440−467.

(5) Polak, E.; Ribiere, G. *Rev. Fr. Inf. Rech. Oper.* **1969**, *16-R1*, 35−43.

(6) Weiner, S. J.; Kollman, P. A.; Case, D. A.; Singh, V. C.; Ghio, C.; Alagona, G.; Profeta, S., Jr; Weiner, P. *J. Am. Chem. Soc.* **1984**, *106*, 765−784.

(7) Still, W. C.; Tempczyk, A.; Hawley, R. C.; Hendrickson, T. *J. Am. Chem. Soc.* **1990**, *112*, 6127−6129.

(8) The geometry adopted by the **BPP34C10** macrocycle in the solid state was employed. For the X-ray crystal structure of **BPP34C10**, see: Allwood, B. L.; Spencer, N.; Shariari-Zavareh, H.; Stoddart, J. F.; Williams, D. J. *J. Chem. Soc., Chem. Commun.* **1987**, 1061−1064.

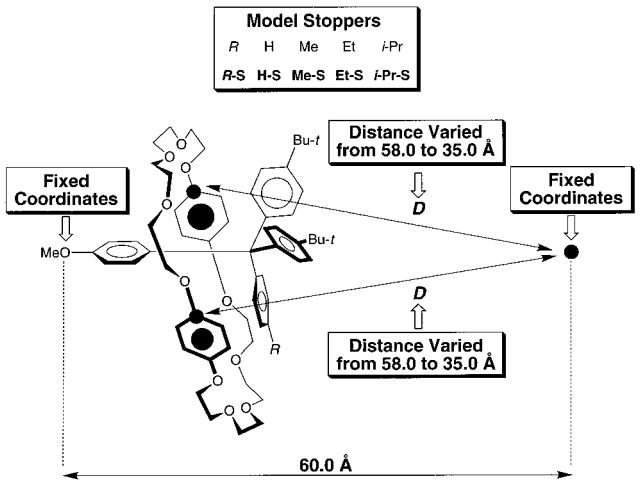

Figure 2. The initial geometry and the constraints employed for simulating the passage of the **BPP34C10** macrocycle over the ***R*-S** model stoppers.

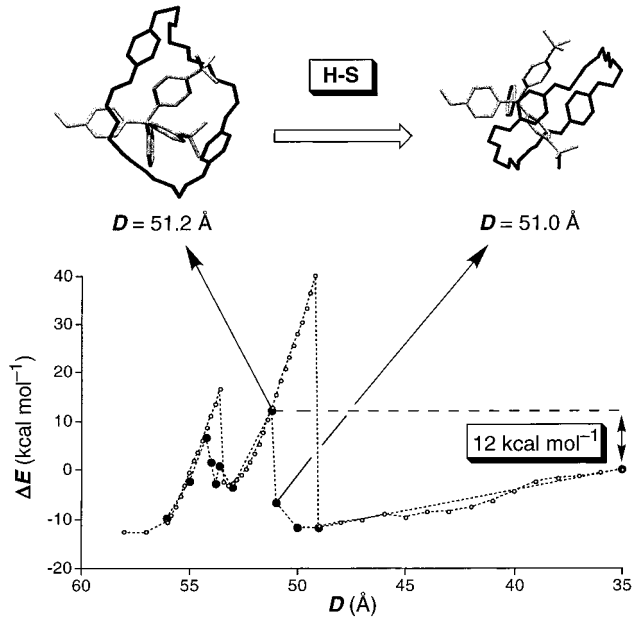

Figure 3. Plots of the relative energies Δ*E*, determined by (○) energy minimization or by (•) energy minimization followed by molecular dynamics and multiconformer minimization, against the distance *D* in the case of the model stopper **H**−**S**.

thus some of the energy-minimized structures obtained between 56.0 and 49.0 Å were subjected individually to molecular dynamics for 20 ps (time step 1.5 fs) at a simulated temperature of 500 K, followed by PRCG minimization of 200 randomly selected conformers to find the lowest energy geometry for each fixed value of *D*. The energies calculated for the lowest energy point obtained for each value of *D* are plotted in Figures 3−6.

Results. The energy profile associated with the slipping-off of the **BPP34C10** macrocycle over the model stopper **H-S** obtained by simple energy minimization at each value of *D* is shown in Figure 3 (symbol ○). Abrupt decreases of Δ*E* are observed after the two energy barriers, suggesting that pathways involving lower energy conformations might be possible. As a result, a second energy profile (•, Figure 3) was derived by energy minimization followed by high-temperature molecular dynamics and subsequent reminimization. Indeed, lower energy conformations were found, and less dramatic Δ*E* drops were obtained. These curves should be good approximations to the

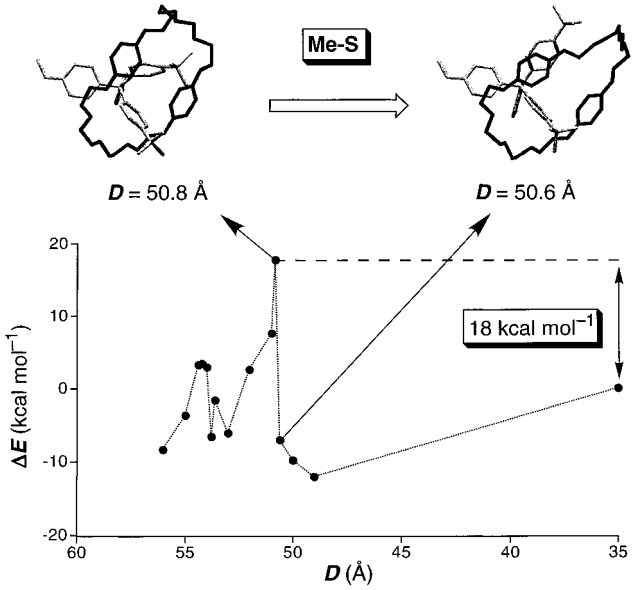

Figure 4. Plots of the relative energies Δ*E*, determined by energy minimization followed by molecular dynamics and multiconformer minimization, against the distance *D* in the case of the model stopper **Me-S**.

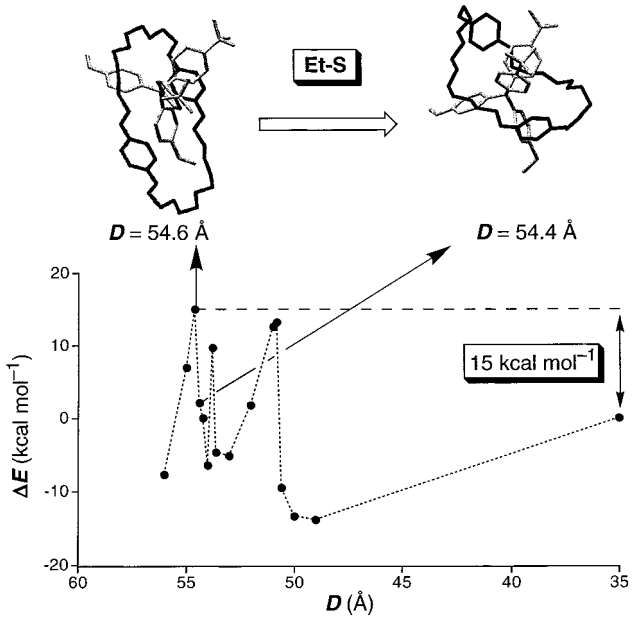

Figure 5. Plots of the relative energies Δ*E*, determined by energy minimization followed by molecular dynamics and multiconformer minimization, against the distance *D* in the case of the model stopper **Et-S**.

lowest energy pathways through the real transition state. The complexity of the potential surface (513 degrees of freedom for ***i*-Pr-S**/**BPP34C10**) prohibits any more exhaustive search of the surface, but we believe this procedure gives approximations to the real transition states

The first energy barrier, occurring between 55 and 53 Å, involves the passage of one of the two polyether chains of **BPP34C10** over the R-C_6H_4- ring; the related motion is illustrated in Figures 5 and 6 for **Et-S** and ***i*-Pr-S**, respectively. The second barrier, occurring between 52 and 50 Å, corresponds to the passage of the other polyether chain of **BPP34C10** over one of the two *t*-Bu-C_6H_4- rings; this motion is illustrated in Figures 3 and 4 for **H-S** and **Me-S**, respectively. The motions involved in this slipping-off resemble those expected for

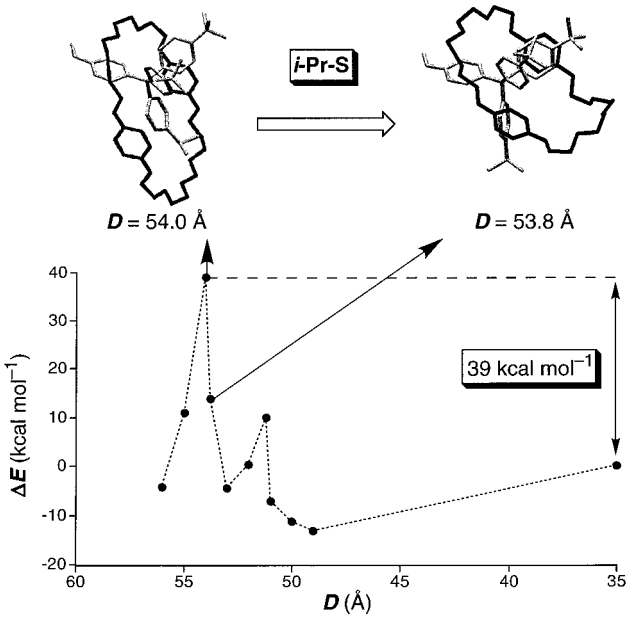

Figure 6. Plots of the relative energies Δ*E*, determined by energy minimization followed by molecular dynamics and multiconformer minimization, against the distance *D* in the case of the model stopper ***i*-Pr-S**.

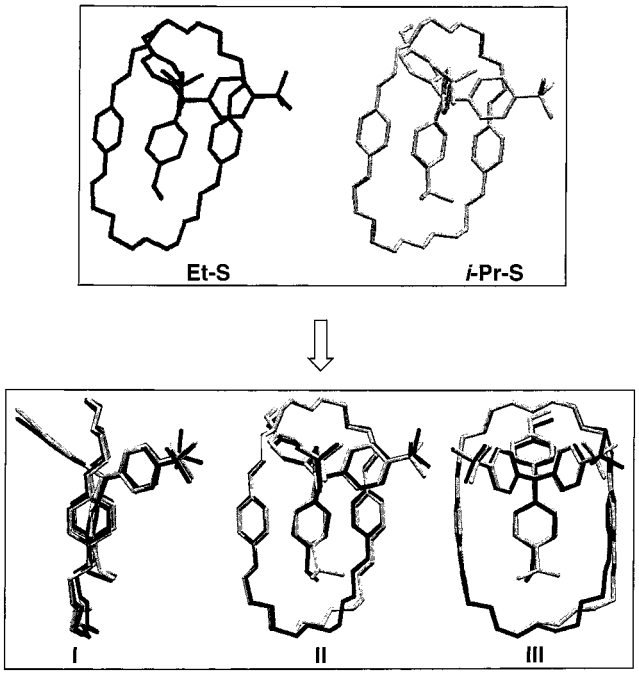

Figure 7. Different views (I−III) of the superimposed "transitions states" found for the slipping-off of **BPP34C10** over the **Et-S** and ***i*-Pr-S**. Note the differences in the conformation of the OCH_2CH_2O linkages facing the *R* group and in the orientation of the *R*-C_6H_4 rings.

dragging a kite out of a tree. The narrowest part of the stopper (kite) pops out of the crown (branches) first, while the two larger substituents get caught on the branches. Further pulling on the string causes significant increase in energy, until the stopper (kite) rotates about 90° to allow the *t*-Bu-C_6H_4- ring to pop through the macrocycle, while the third *t*-Bu-C_6H_4- group is still caught against the macrocyclic polyether (tree branches). Once only the last *t*-Bu-C_6H_4- ring remains, it is pulled through the macrocycle with essentially no barrier.

Similar energy profiles, showing two main energy barriers, were also located (Figures 4−6) for the model stoppers **Me-S**, **Et-S**, and ***i*-Pr-S**. In the case of **H-S** and **Me-S** (Figures 3 and 4, respectively), the rate determining step is the second one and the corresponding calculated energy barriers[9] are 12 and 18 kcal mol^{-1}, relative to the energy of the separated entities. By enlarging the *R* group, the first energy barrier increases relative to the second one. Indeed, in the case of **Et-S** and ***i*-Pr-S** (Figures 5 and 6, respectively), the rate determining step becomes the first one. However, while the energy barrier calculated for **Et-S** in only 15 kcal mol^{-1}, a value comparable with those determined for **H-S** and **Me-S**, the energy barrier derived for ***i*-Pr-S** (39 kcal mol^{-1}) *is more than twice that of any other stopper!* The trend in these calculated energy barriers is in very good agreement with the trend in the experimental yields of the corresponding [2]rotaxanes (Figure 1); *in both cases, a dramatic change is observed on going from Et to* i-*Pr*. This substituent effect is a result of large steric repulsions between the *R* group and one of the polyether chains of the **BPP34C10** macrocycle. Figure 7 provides a comparison of the geometries of the rate-determining "transition states" determined for the slippage over **Et-S** and ***i*-Pr-S**. The subtle differences embodied in the two transition states lead to the 24 kcal mol^{-1} increase in the activation energy for the passage of the *i*-Pr-C_6H_4- ring as compared to the Et-C_6H_4- ring. The motions involved in both cases involve the anchoring of the (*t*-Bu-$C_6H_4)_2C$ moiety near the "top" of **BPP34C10** and the movement of the *R*-C_6H_4- ring through its cavity. The rectangular shape of **BPP34C10** leaves ample room for the passage of the Et group. By contrast, the macrocyclic polyether and the *i*-Pr-C_6H_4- ring must distort to allow the *i*-Pr group to swing through. This is especially apparent in superimpositions II and III (Figure 7). The side view (I) shows how the *i*-Pr-C_6H_4- ring is bent, because the methyl groups are clashing with the polyether chain. This may also be seen in views II and III, where the increase of the **BPP34C10** diameter by torsional and angle adjustments of the polyether chain permits the *i*-Pr group to pass through. Single point AMBER* calculations of the energies of the **BPP34C10** components of the transition states shown in Figure 7 revealed an increase of 6 kcal mol^{-1} when *R* is equal to *i*-Pr. The increase of the energy of the stopper component of the transition state relative to the global minimum of the free stopper is 15 kcal mol^{-1} higher for that of *R* equal to *i*-Pr. Thus, both the distortions of the macrocycle and of the stopper contribute to enhance the energy barrier for the slipping-off over ***i*-Pr-S** with the latter being the dominant factor.

Conclusions

To gain further understanding into the mechanism and the size complementarity requirements associated with the slippage approach to rotaxanes, we have carried out a computational investigation employing the **BPP34C10** macrocycle and tetraarylmethane-based model stoppers ***R*-S** differing in the size of the *R* group. These computational simulations have revealed two main energy barriers for the slipping-off of the **BPP34C10** macrocycle over the ***R*-S** stoppers. The first one involves the passage of the macrocycle over the *R*-C_6H_4- ring, while the second one is associated with the slippage over one of the two *t*-Bu-C_6H_4- rings. When *R* is equal to H or Me, slippage over the first ring is easy, and the second energy barrier, namely, the passage over a *t*-Bu-C_6H_4- ring, is dominant. When *R* is equal to Et or *i*-Pr, however, the passage over the *i*-Pr-C_6H_4-

(9) In analogous systems, the free energies of activation determined (ref 1f and g) experimentally for the slipping-on and slipping-off processes range from 20 to 25 kcal mol^{-1}. The enthalpic terms of these free energies of activation range from 10 to 21 kcal mol^{-1}.

ring becomes rate-determining. The energy barrier calculated for ***i*-Pr-S** (39 kcal mol^{-1}) is more than two times higher than any of those calculated for the other ***R*-S** stoppers, which are all lower than 20 kcal mol^{-1}. The trend in the calculated energy barriers is in very good agreement with the experimental yields of the corresponding [2]rotaxanes, and in both cases, a remarkable change is observed on going from Et to *i*-Pr. This abrupt substituent effect is a result of steric hindrance between the bulky *i*-Pr group and one of the polyether chains of the **BPP34C10** macrocycle.

Acknowledgment. This research was supported by the Engineering and Physical Sciences Research Council (J.F.S.) and the National Institute of General Medical Sciences, National Institutes of Health (K.N.H.).

JA9806229